Microsyst Technol (2011) 17:923–929
DOI 10.1007/s00542-010-1187-5

TECHNICAL PAPER

A thin multi-ring negative liquid crystal lens enabled by high-κ dielectric material

Chao-Jui Hsu · Paul C.-P. Chao · Yung-Yuan Kao

Received: 31 August 2010 / Accepted: 16 December 2010 / Published online: 5 January 2011

Abstract This study is dedicated to design an liquid crystal (LC) negative lens with unequal width electrodes, which is made for a camera lens and with the aim to replace conventional negative lenses. The structure of the LC negative lens is symmetric for producing a symmetrical electric field. The unequal widths are adopted and determined inversely proportional to the slopes of the desired applied voltages at varied radial positions. There are four ring electrodes in the lens and the associated with applied different voltages. In addition, the performance of the designed LC lens is verified by the software DIMOS.2D. The special structure and the material are used to realize the designed LC lens. Moreover, a new fabrication process in the wafer level to bury bus lines is developed in order to smooth the generated electric field distribution. In addition, a high-κ dielectric layer is coated between the electrodes and the LC layer for minimizing required applied voltage. Finally, differential effects of the LC lens structure with high-κ and without high-κ are discussed based on simulation results.

1 Introduction

Liquid crystal lens molecules are known of substantial optical and electrical anisotropies such that the refractive indexes along different directions across a molecule are different and can be easily changed by molecule rotations. These LC rotations can be attained by applying different voltages across the LC molecules. The earliest presentation of the relationships among effective refractive indices, gestures of LC molecules, and electric fields was proposed in Deuling (1972). An LC lens with a lens-shaped cell was proposed about 30 years ago (Sato 1979). Most of the proposed LC lenses are optical positive lenses. The hole-typed negative LC lens has been designed by Sato in 2005 (Wang et al. 2005). There were lenses using in positive and negative (Wang et al. 2006; Ye et al. 2008). Generating a particular electric field across the LC cell by applying required voltages, the proposed LC lens and its electrodes are able to offer a gradient index distribution over the aperture such that it acts like a gradient refraction index (GRIN) lens with a quadratic-like index distribution. All the studies were devoted for a better index distribution as close as possible to the GRIN lens (Kraan et al. 2007; Kurihara and Hashimoto 2006; Kao et al. 2009). Some works used high resistance materials to form the electrodes (Valley 2007; Kao et al. 2010), while others used two LC layers (Valley et al. 2010).

A new method of designing the LC negative lens with multi-ring electrodes in unequal widths and the associated with new fabrication process is proposed in this study. In order to mimic the perfect negative GRIN lens, generating the particular electric field and refractive index distribution are important. Thus, in this study, the negative LC lens is designed to own multiple electrodes. To render required electrical field by finite multiple ring electrodes, the number and widths of electrodes are determined by the slopes of the required applied voltage in different positions. Furthermore, in order to generate desired electrical fields in a thin LC lens, a dielectric high-κ material, as initially proposed by Loktev et al. (2007), is coated between the LC and the electrodes layers to smooth out the desired index distribution. Finally, a new fabrication process is developed to bury

C.-J. Hsu · P. C.-P. Chao (✉) · Y.-Y. Kao
Department of Electrical Engineering, National Chiao Tung University, Hsinchu 300, Taiwan
e-mail: pchao@mail.nctu.edu.tw

P. C.-P. Chao
Institute of Imaging and Biophotonics, National Chiao Tung University, Tainan, Taiwan

the bus lines under the ring electrodes, in order to avoid undesired electric field distortion near the bus lines.

2 Design principles

A GRIN lens owns the refractive index distribution in a particular gradient manner along the radial direction of the lens, the principle of which is applied to an LC lens. Based on the principle, a desired focal length of the LC GRIN lens f can be achieved, yielding

$$f = \frac{r^2}{2d \cdot [n(r)_{\min} - n(r)]}, \tag{1}$$

where r, d, $n(r)_{\min}$, and $n(r)$ are radius, thickness, minimum refractive index, and the index distribution of LC lens along the radial direction, respectively. In our design, the material of LC is E7, of which n_e, the extraordinary refractive index, is 1.7371; n_o, the ordinary refractive index, is 1.5183. Thus, the maximum difference between two indices of refraction. $\Delta n_{\max}$ is 0.2188 for the 633 nm wavelength. The radius of lens aperture is considered as large as $r = 2.5$ mm, while the cell gap of the LC lens is chosen as $d = 50$ μm. In the results, the LC lens reaches a focal length f of −286 mm. On the other hand, Eq. 1 could be rewritten as

$$n(r) = n(r)_{\min} - \frac{r^2}{2fd}. \tag{2}$$

Calculating from Eq. 2, the function and figure of distribution of index refraction $n(r)$ of GRIN negative lens versus r are shown in equation below and Fig. 1, respectively,

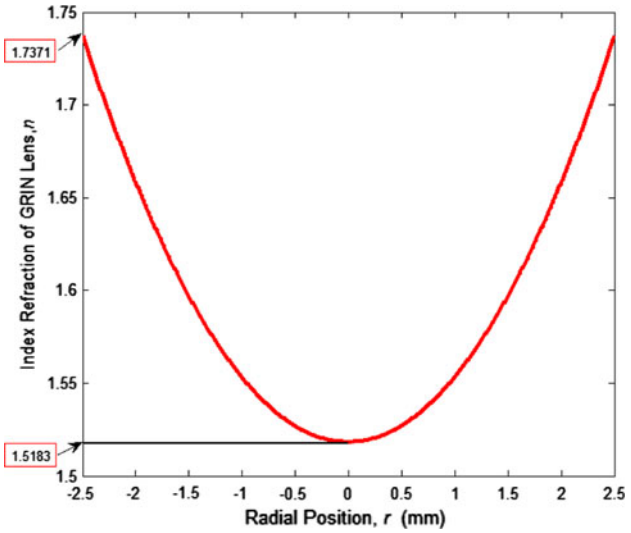

Fig. 1 Illustration of perfect refractive index n for GRIN lenses versus r

$$n(r) = 1.5183 + 0.035008r^2. \tag{3}$$

The orientation of the nematic liquid crystals in an electric field between two electrode plates is shown in Fig. 2. By Huygens method (Sluijter et al. 2009), the effective refractive index of LC lens, n_{eff}, can be calculated by the effective tilting angle ϕ_{eff} in

$$n_{eff}(\phi_{eff}) = \frac{n_o n_e}{\sqrt{n_e^2 \cos^2 \phi_{eff} + n_o^2 \sin^2 \phi_{eff}}}, \tag{4}$$

where ϕ_{eff} is the angle relative to perpendicular. In order for the LC lens to mimic GRIN negative lens, Eq. 4 should equal Eq. 3 along the LC lens radius r. After calculation, the relation between ϕ_{eff} and r is shown in

$$\phi_{eff}(r) = \cos^{-1}\left[n_o \sqrt{\frac{\left[n_e^2 \Big/ (1.5183 + 0.035008r^2)^2 \right] - 1}{(n_e^2 - n_o^2)}} \right]. \tag{5}$$

Based on Eq. 5, the relation between the refractive index distribution and the tilting angle ϕ_{eff} for a perfect GRIN negative lens versus r is illustrated by Fig. 3.

Applying a certain voltage to the LC layer between two electrode plates, the required tilting angle of LC molecules for the perfect GRIN lens can be calculated by Deuling (1972),

$$V = V_o \frac{2}{\pi} \sqrt{1 + \Upsilon \cos^2 \phi_m} \int_0^{\phi_m} \left\{ \frac{1 + \kappa \cos^2 \phi}{(1 + \Upsilon \cos^2 \phi)(\cos^2 \phi_m - \cos^2 \phi)} \right\}^{1/2} d\phi, \tag{6}$$

where V, V_o, and Φ_m are applied voltage, threshold voltage and maximum tilting angle at the center of LC layer, respectively. The parameters of V_o, κ, and γ are represented as

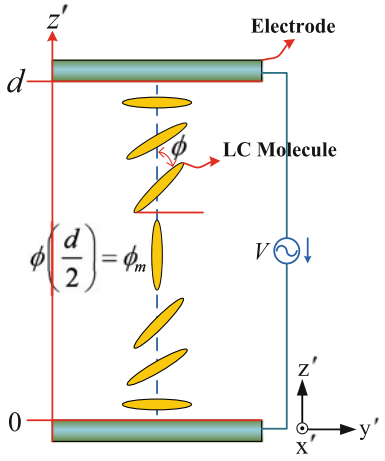

Fig. 2 The orientation model for nematic liquid crystal molecules rise from the substrate by the electric field

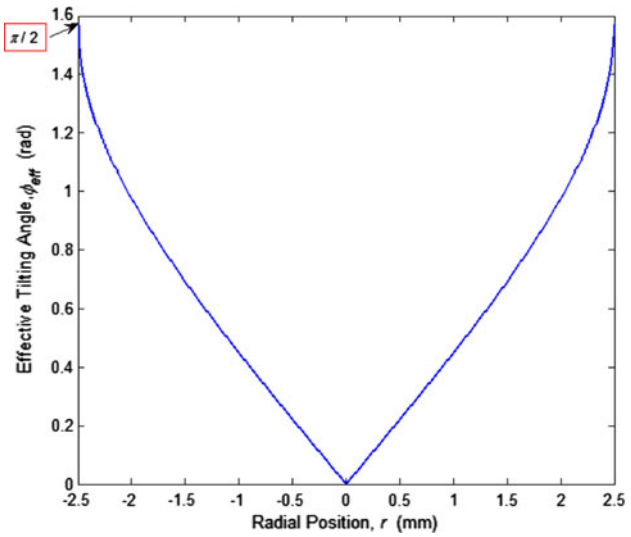

Fig. 3 The perfect effective tilting angle Φ_{eff} for GRIN lenses versus r

$$V_o = \pi \left[\frac{K_{11}}{\varepsilon_o (\varepsilon_{\parallel} - \varepsilon_{\perp})} \right]^{1/2}, \tag{7}$$

$$\gamma = \frac{\varepsilon_{\parallel} - \varepsilon_{\perp}}{\varepsilon_{\perp}}, \tag{8}$$

$$\kappa = \frac{K_{33} - K_{11}}{K_{11}}, \tag{9}$$

where $\varepsilon_{\parallel}$, $\varepsilon_{\perp}$, K_{11}, and K_{33} are the relative dielectric permittivity parallel to the director of LC molecules, the relative dielectric permittivity perpendicular to the director of LC molecules, the elastic curvature constants of splay and the elastic curvature constants of bend, respectively.

To determine the widths of the four ring electrodes, the process of which is started with designing the electrode widths as inverse proportional to slopes of the applied voltages, as illustrated by the chart in Fig. 4. First, the radius is divided into four parts which have the relative slopes, m_i's, of every part calculates by $(V_i - V_{i+1})/0.625$, where $i = 1$–4. V_1–V_5 are calculated by the software MATLAB, 5.5, 1.93, 1.45, 1.1, and 0.9 V, respectively. Second, m_1, the slope of the most inner electrode is set to be the reference for determining other four electrode widths by a inverse fashion, following

$$\frac{w_i}{w_1} = \frac{m_1}{m_i}, i = 1, 2, 3, 4. \tag{10}$$

Note that for a negative LC lens, the most inner electrode with width w_1 is applied with the largest voltage, therefore based on Eq. 10 w_1 is the smallest in four ring electrode widths. w_1 is in fact determined by the process of fabrication. This smallest width of fabrication w_1 is 35 μm.

The four electrodes, ring1, ring2, ring3, and ring4, are placed on the radial positions, 0, 0.83, 1.67, and 2.5 mm,

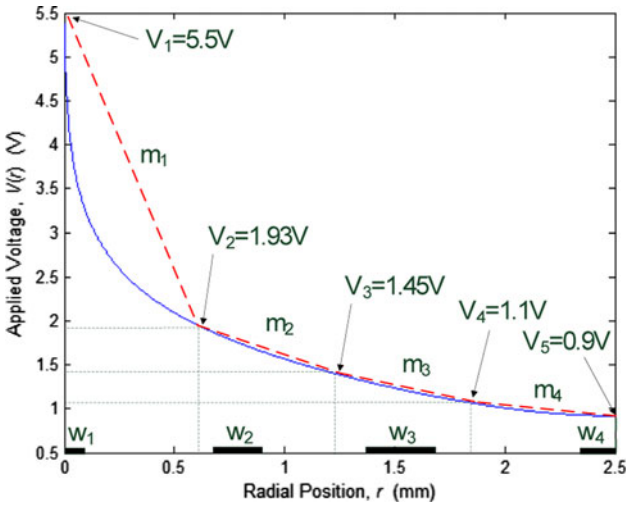

Fig. 4 The relation between applied voltage, $V(r)$ and radial position, r

Table 1 The designed properties, slopes and unequal width, of the multi-ring LC lens

Ring	Slope, m	Width, w (μm)
1	5.76	35
2	0.864	250
3	0.416	500
4	0.32	150

respectively, as shown in Fig. 4. After calculation, m_1, m_2, m_3, and m_4 are 5.76, 0.864, 0.416, and 0.32. The resulting m_1/m_2, m_1/m_3, and m_1/m_4 are 6.67, 13.85, and 18, respectively. The ring widths, w_1, w_2, w_3, and w_4, are about 35, 250, 500, and 650 μm, respectively. Since the aperture is only 2.5 mm, w_4 is cut to be 150 μm. The slopes and widths of four rings are shown in Table. 1. The illustrations, top view and end view of the LC negative lens are shown in Fig. 5a, b, respectively.

3 Proposed fabrication process

The structure and fabrication process of the unequal width ring electrodes on a glass substrate for the proposed LC lens are stated in the followings. Based on the previous principle, four ITO transparent electrodes in ring type as marked in blues in Fig. 6a, b are considered in the current study to verify the proposed LC lens design. Figure 6a depicts the traditional design of mask where extensions of electrodes (e.g., bus lines) across rings are present, in order to apply varied voltages to each electrodes. This baseline design is implemented by the structure as shown in Fig. 5b, where two glass substrates in thickness is 550 μm and coated with ITO ring electrodes pattern in 450 Å thickness are expected to be combined with a gap filled with liquid

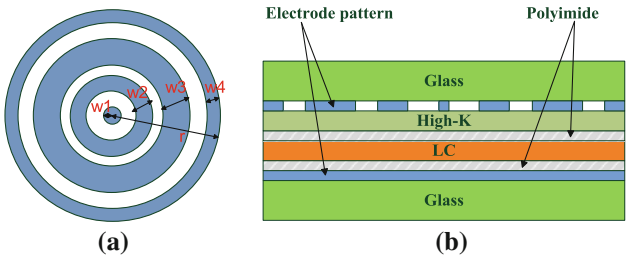

Fig. 5 **a** The *top view* pattern of the unequal width LC lens. **b** The *end view* of the unequal width LC lens

crystals. The ITO electrode owns, based on measurement, a transmittance of 94%. On the tops of the two patterned ITO glass substrates, polyimide (PI) layers (AL-1426B, from Daily-Polymer Corp.) are coated for insulation and implementing rubbing. Both PI layers are rubbed to form the micro-grooved surfaces, leading to LC tilts of 2°, in order to smooth away the disclination effect. The two layers of PI are then stacked with 50 μm Mylar spacer in between. The LC E7 from Merck is filled in the gap between the two glass substrates, thus the thickness of E7 is 50 μm. In addition, a layer of high-κ material is inserted between the PI and ITO to render, as stated previously, smoother electrical field gradients.

The four ring electrodes in the afore-designed LC GRIN lens structure are, as shown in Fig. 5a, in the same ITO layer. It is inevitable to extend the electrodes to cross rings to form bus lines for applying external voltages, as shown in Fig. 6a. These bus lines (crossing extensions of electrodes) would definitely cause undesired electric fields in its local area and then result in unexpected LC rotations. In addition to the afore-mentioned problem, it is also reported from Valley (2007) and Kao et al. (2010) that the space between adjacent electrode rings ought to be large enough

Fig. 6 **a** The electrode pattern with all electrodes in the same layer, **b** with buried *bus lines*, **c** the fabrication process for ring electrodes and buried *bus lines*

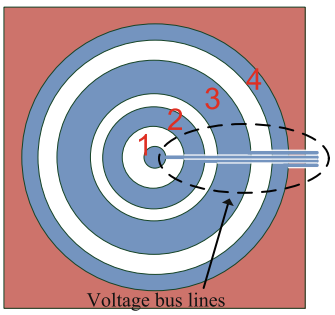

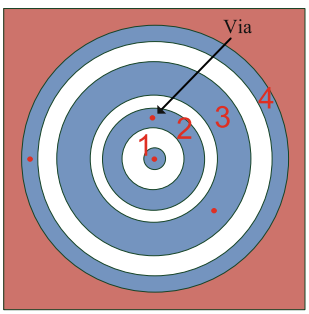

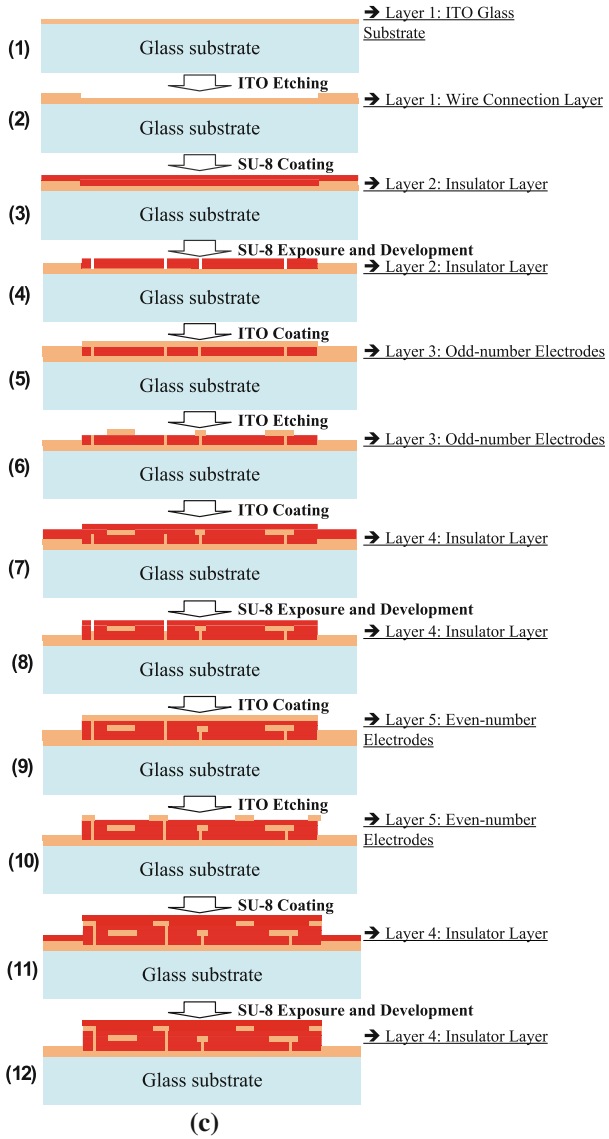

to avoid possible effects of short cuts. To remedy the above-problems, a new structure and associated fabrication process are proposed in this study, as illustrated by Fig. 6b, c, respectively. In this fabrication process, the odd- and even-numbered electrodes are deposited and patterned at two different layers and separated by an insulator SU-8. In this way, as those red dots depicted in Fig. 6b, the bus lines are buried below the layer of ring electrodes.

The details for fabricating different layers of electrodes are illustrated by Fig. 6c and stated in the followings. First, from (1) to (2), the ITO layer is patterned for the bus lines of all electrodes. These electrode bus lines are in radial extension to the outmost region of the glass substrate to be wire bounded. They do not cross each other in this layer. From (3) to (7), odd-numbered electrodes are formed with the ITO VIA holes connected the foundation and capsulated by insulating SU-8, which thickness is about 1 μm. Step (8) exposes the electrode pad for wire bounding. Steps (9) to (11) are for even-numbered ring electrodes. Also, Step (12) exposes the electrode pads for even-numbered rings to be wire bounded. By this design, the bus lines are buried below the conducting electrode rings such that the ring electrodes without crossing bus lines as shown in Fig. 6b can be realized. The distortions of electric fields in the local area around the bus lines as shown in Fig. 6a are avoided. Another advantage is that the neighboring electrodes need no spacing and the upper even-numbered electrodes could even be a little wider than originally designed in order to avoid over-etching in the process and also control the resistance to a lower value for a fast response.

4 Simulation results and discussion

The optical performance of the afore-proposed design principles of the thin negative LC lens is verified by software DIMOS.2D from AUTRONIC MELCHERS. The software is able to calculate the electro-optical properties of LC lenses in the two spatial dimensions that define a cross-section through the LC lens. In this study, two structures are designed and considered to analyze the lens performances with high-κ layer and non-high-κ layer. The essential properties of the proposed lens are unequal width electrodes, high-κ material layer, LC layer and a plane electrode in the simulation. Besides, the thicknesses of the unequal width electrodes, high-κ material layer, LC layer and plane electrode are 20, 100, 50, and 20 μm, respectively, as shown in Fig. 7a, while Fig. 7b is the design without high-κ layer. The LC material, E7 from Merck, fills the gap between the high-κ layer and the plane electrode. E7 adopted herein owns the ordinary refractive index n_o, of 1.5183 while the extraordinary refractive index, n_e of

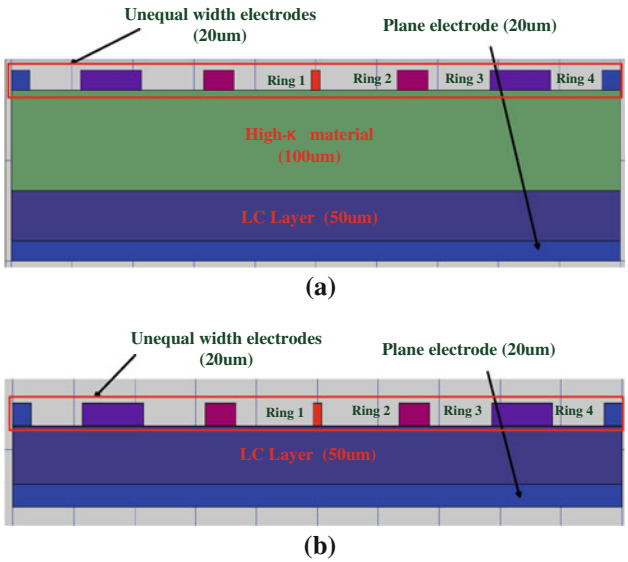

Fig. 7 Structure of simulation in DIMOS.2D **a** with high-κ, **b** without high-κ

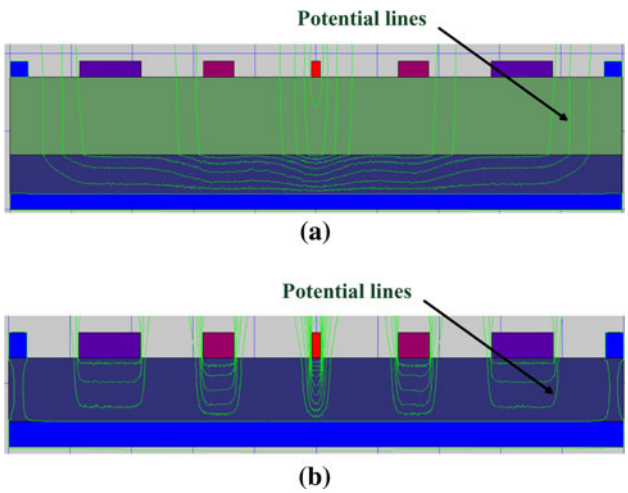

Fig. 8 *Potential lines* of simulating result **a** with high-κ, **b** without high-κ

1.7371 for the light with 633 μm wavelength. The associated elastic constants K_{11}, K_{22}, and K_{33} are 11.1, 5.9, and 17.1 pN, respectively. The permittivities $\varepsilon_{\parallel}$ and $\varepsilon_{\perp}$ are 19.28 and 5.21, along parallel and perpendicular directions, respectively. Finally, the rotational viscosity is 233 m-Pa.

Figures 8 shows the simulation results by DIMOS.2D—the electrical equipotential lines of the two structures with suitable driving voltages. The equipotential lines, affecting the orientation distribution of the LC molecules, are presented a distribution of gradient through a high-κ layer, as shown in Fig. 8a. In addition, it is clearly seen from Fig. 8b that the equipotential lines are discontinuous with the applied voltages from the unequal width electrodes to the LC layer directly, rendering non-smooth-gradient distribution

of equipotential lines in this structure. Thus, the refractive index distribution of the equipped high-κ layer structure is more continuous and smooth in gradient than the one without high-κ layer structure equipped. In results, the negative LC lens owns a better chance to approach the focusing effects mimicking a perfect GRIN lens.

With equipotential lines simulated by DIMOS.2D, the steady-state LC molecules are next simulated by a DIMOS model that cuts the LC layer into 120 spits and 20 slabs, in order to simulate steady-state tilting angles of LC molecules. The deformation profiles of the LC tilting angles are then exported from DIMOS.2D. Finally, the simulated tilting angles of each LC spit are averaged by a MATLAB program and substituted into Eq. 4 to calculate the effective index distribution of refraction. The index data from simulation for the lens designs with high-κ and non-high-κ material layers are fitted in a quadratic polynomial by a MATLAB program, as shown in Fig. 9. In the figures, the triangles denote the resulted indices from simulation. The dash lines are the perfect refractive index distribution for a perfect GRIN negative lens, while the solid line results from the curve fitting of the refractive indices based on DIMOS simulations. Figure 9a depicts the refractive index distribution in the structure with a high-κ layer. The fitted curve of the distribution is also shown in this figure, in order to be compared with the perfect refractive index and the simulation result. The function of the fitted curve is

$$n(r) = 0.03269r^2 - 0.0003827r + 1.554$$

and the calculated root mean square error (RMSE) is 0.01462. Moreover, the focal length of the perfect GRIN negative lens is -286 mm, while the proposed GRIN lens is -307 mm, indicating that the designed and fabricated negative LC lens has the ability to render a negative focus length close to that of a GRIN lens counterpart. As for Fig. 9b where no high-κ layer is adopted, the refractive index distribution is highly irregularly distributed, especially around the unequal width electrodes, leading to the fact that the lens without high-κ layer is not able to mimic well a GRIN negative lens. Therefore, the simulation with high-κ material layer is much more capable to behave like a negative focusing lens than without high-κ material.

5 Conclusion

An LC negative lens with unequal electrode widths and high-κ material layer has been successfully designed in this study. It is driven by different voltages on every electrode. Base on this design, the LC negative lens with unequal electrode widths has been simulated. The fabrication process of the LC lens has been designed. Distribution of the refractive index in the structure with high-κ mimics well the proposed LC lens and much more capable to behave like a negative focusing lens than without high-κ material. Experimental studies will be conducted to measure real EFL and PSF in the future.

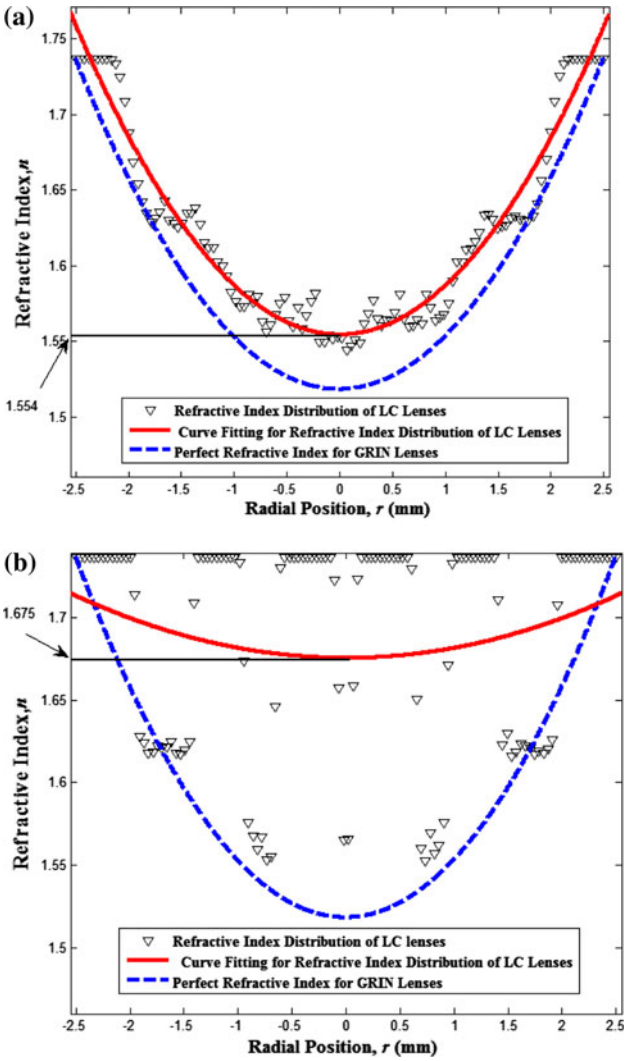

Fig. 9 *Curve* fitting of simulating result **a** with high-κ, **b** without high-κ

Acknowledgments The authors are indebted to the National Science Council, Taiwan, under the contracts NSC 98-2220-E-009-018 for their financial supports. Furthermore, authors are also indebted to the National Nano Device Laboratories of Taiwan.

References

Deuling HJ (1972) Deformation of nematic liquid crystals in an electric field. Mol Cryst Liq Cryst 19:123–131

Kao Y-Y, Huang Y-P, Yang K-X, Chao PC-P, Tsai C-C, Mo C-N (2009) An auto-stereoscopic 3D display using tunable liquid crystal lens array that mimics effects of GRIN lenticular lens array. In: 2009 SID international symposium digest of technical papers XL: 111–114

Kao Y-Y, Chao Paul C-P, Hsueh C-W (2010) A new low-voltage-driven GRIN liquid crystal lens with multiple ring electrodes in unequal widths. Opt Exp 18:18506–18518

Kraan TC, van Bommel T, Hikmet RAM (2007) Modeling liquid-crystal gradient-index lenses. J Opt Soc Am 24:3467–3477

Kurihara M, Hashimoto N (2006) Liquid crystal optics for laser beam modulation. Proc SPIE 6374:U101–U106

Loktev M, Vdovin G, Klimov N, Kotova S (2007) Liquid crystal wavefront corrector with modal response based on spreading of the electric field in a dielectric material. Opt Exp 15:2770–2778

Sato S (1979) Liquid-crystal lens-cells with variable focal length. Jpn J Appl Phys 18:1679–1684

Sluijter M, Herzog A, de Boer DKG, Krijn MPCM, Urbach HP (2009) Ray-tracing simulations of liquid-crystal gradient-index lenses for three-dimensional display. J Opt Soc Am B 26:11

Valley P, Li G, Äyräs P, Mathine DL, Honkanen S, Peyghambarian N (2007) High-efficiency switchable flat diffractive ophthalmic lens with three-layer electrode pattern and two-layer via structures. Appl Phys Lett 90:111105-1–111105-3

Valley P, Mathine DL, Dodge MR, Schwiegerling J, Peyman G, Peyghambarian N (2010) Tunable-focus flat liquid-crystal diffraction lens. Opt Lett 35:336–338

Wang B, Ye M, Sato S (2005) Liquid crystal negative lens. Jpn J Appl Phys 44(7A):4979–4983

Wang B, Ye M, Sato S (2006) Liquid crystal lens with focal length variable from negative to positive values. IEEE Photonics Technol Lett 18:1

Ye M, Wang B, Sato Y, Kawamura M, Yamaguchi R, Sato S (2008) Transient properties during positive–negative switching of liquid crystal lens. Mol Cryst Liq Cryst 480:44–48